Check for updates

Host–guest chemistry of tridentate Lewis acids based on tribenzotriquinacene†

Maurice Franke, [ID] Tobin Ens, Andreas Mix, [ID] Beate Neumann, Hans-Georg Stammler [ID] and Norbert W. Mitzel [ID] *

Flexible poly-Lewis acids (PLA) based on the tribenzotriquinacene (TBTQ) scaffold have been synthesised. Hydrosilylation of 4b,8b,12b-triallyltribenzotriquinacene and subsequent exchange of the chlorine substituents with weaker coordinating triflate groups afforded a novel triple silyl-functionalised PLA. By regioselective hydroboration of triallyl–TBTQ with various organoboranes, PLAs with different Lewis acidities were obtained. The synthesised PLAs were combined with neutral bases in host–guest experiments. DOSY NMR spectroscopy was performed to elucidate the complexation process in solution. These experiments revealed a highly dynamic interaction between the boron-functionalised PLA and triazine. However, the addition of one equivalent of tris(dimethylphosphino(methyl))phenylsilane led to the formation of a 1 : 1 adduct, which was confirmed by diffusion experiments.

Introduction

Host–guest chemistry has become an extensively studied area of supramolecular chemistry since Pedersen's publication of crown ether–potassium complexes.[1] Crown ethers consist of several linked Lewis base functions and are therefore called poly-Lewis bases. In contrast, the less well studied poly-Lewis acids consist of several Lewis acid functions linked to an organic backbone. A useful distinction is that between (semi-)flexible,[2] rigid[2e,3] and cyclic[2e,4] PLAs, as the flexibility influences the complexation potential towards Lewis base guest molecules. While rigid PLAs are able to recognise molecules of a specific size[3c,d,5] due to the defined spatial arrangement of the Lewis acid functions, PLAs with more flexible spacing are accessible to a greater variety of Lewis bases and subsequent transformations.

Besides mercury,[4c,6] silicon[2d,7] and tin,[2e,3e,4d] the elements of the third main group (B,[2b,c,3b,d,5b,c,8] Al,[9] Ga,[10] In[11]) are often used as acceptor sites. Today, there are various examples of organic backbones with different properties of the resulting PLAs. Previous work in the field of poly-Lewis acids by our group included the Lewis acid functionalisation of the trisila-cyclohexane scaffold[7d,8a,10e,g] and extensive studies of the anthracene molecule[5c,7c,9c,d,11b,12] as backbone for bi- and tetradentate poly-Lewis acids as well as for poly-pnictogen-bonding host-systems,[13] which are the subject of current research. Recently, we reported on the preparation of novel derivatives based on C_{3v}-symmetric tribenzotriquinacene (TBTQ)[14] which was first synthesised by Kuck *et al.* in 1984.[15] We introduced various silyl substituents *via* Grignard reactions and hydrosilylation. However, the attached Lewis acid functions showed no reactivity towards Lewis basic donor molecules, due to the low Lewis acidity of the silyl functions, as we already observed for other bi- and tridentate silicon-based poly-Lewis acids.[2c,7a,c,e] Although fluoride ions were readily complexed with trifluorosilyl-substituted PLAs,[2d] no further reactions with Lewis basic molecules such as pyridine were observed. Synthetic protocols to increase the Lewis acidity of silicon atoms by introducing electron-withdrawing groups have been reported by Greb *et al.* with the synthesis of bis(catecholato)silanes.[16] After the introduction of weakly coordinating anions such as carboranes[17] and triflate[18] silicon atoms also exhibited an increased Lewis acidity, which has found application in organic catalysis. Recently, we reported the reactivity of bidentate silyl–triflates in host–guest chemistry.[7b] Diffusion NMR experiments provided insight into host–guest aggregation in solution. Comparison of the diffusion coefficients of the corresponding PLA, the Lewis base and the formed adducts provides detailed information about the aggregate.[12a,16b,19] However, due to the complexity of aggregation in solution it is still difficult to make a statement about the composition of the adducts. Further elucidation by X-ray diffraction experiments provides information about the consti-

Universität Bielefeld, Fakultät für Chemie, Lehrstuhl für Anorganische Chemie und Strukturchemie (ACS), Centre for Molecular Materials (CM2), Universitätsstraße 25, D-33615 Bielefeld, Germany. E-mail: mitzel@uni-bielefeld.de; https://www.uni-bielefeld.de/fakultaeten/chemie/ac3-mitzel/

tution in the solid phase. In this work we present the synthesis of a silyl–TBTQ derivative with increased Lewis acidity, similar to that we previously reported. In addition, we present novel boron-functionalised poly-Lewis acids and their application in host–guest chemistry.

Results and discussion

Syntheses of tridentate poly-Lewis acids

The triallyl–TBTQ compound **1**, that is required for subsequent reactions was prepared according to literature data by a SnCl$_4$ catalysed reaction of 4b,8b,12b-tribromotribenzotriquinacene with allyltrimethylsilane.[20] The following hydrosilylation reaction was carried out in analogy to the reaction conditions we used in previous work to obtain the silyl–TBTQ derivative **2**.[14] Conversion with silver triflate in the absence of light afforded the triflate substituted TBTQ derivative **3** (Scheme 1).

Both products **2** and **3** were obtained as colourless solids in good yields (84%) and were characterised by multinuclear NMR spectroscopy, sc-XRD and elemental analysis. The ^{1}H NMR spectrum proved the regioselectivity of the hydrosilylation reaction and the formation of the anti-Markovnikov

product **2**. The chemical shift of 31.2 ppm in the ^{29}Si{^{1}H} NMR spectrum is consistent with previously synthesised TBTQ–silyl compounds. A single crystal of **2** suitable for X-ray diffraction experiments was obtained, by cooling a saturated solution of **2** in n-hexane to −30 °C (Fig. 1). The molecular structure of **2** confirms the triple hydrosilylation of triallyl–TBTQ **1**. The spatial arrangement of the silyl substituents results in a chalice-shaped molecule.

After reaction with silver triflate, all ^{1}H NMR signals are low-field shifted compared to the corresponding signals of compound **2**. This is in agreement with the ^{29}Si{^{1}H} chemical shift of 43.9 ppm observed for **3**. In contrast to **2**, which is surprisingly stable to air and moisture, the rapid formation of trifluoromethanesulfonic acid, evident from ^{1}H NMR spectra, shows the hydrolysis sensitivity of **3**. Single crystals were obtained by cooling a saturated solution of **3** in n-hexane to −30 °C and were analysed by X-ray diffraction (Fig. 2).

The molecular structure of **3** confirms the triple exchange of the chloro substituents with triflate groups. The bond Si(3)–O(7A) (1.688(7) Å) is significantly shorter than the bonds Si(1)–O(1) and Si(2)– O(4A) (1.754(5), 1.769(6) Å). The distance Si(3)···O(5A) is 3.612(9) Å, just within the sum of the van der Waals radii (r_{vdW}(Si) + r_{vdW}(O) = 3.62 Å).

The hydroboration reaction is a well-established way of functionalising the organic backbone with Lewis acidic borylgroups. To investigate the effect of Lewis acidity and steric demand in host–guest chemistry, we synthesised different tridentate boron Lewis acids. PLA **4** was obtained by conversion
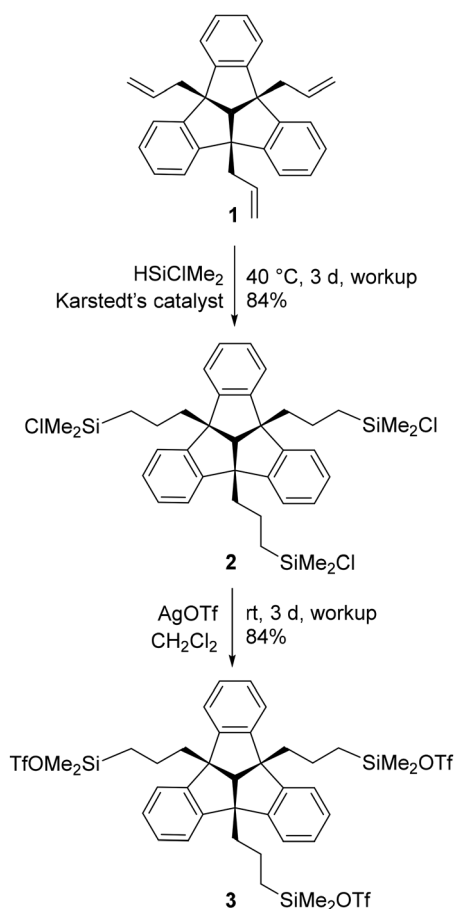
Scheme 1 Syntheses of the trisilyl–TBTQ compounds **2** and **3**, starting from triallyl–TBTQ **1**.

Fig. 1 Molecular structure of **2** in the crystalline state. Displacement ellipsoids are drawn at the 50% probability level. Hydrogen atoms and minor occupied disordered parts are omitted for clarity. For further details, see the ESI.† Selected bond lengths [Å] and angles [°]: C(1)−C(2) 1.563(2), C(2)−C(23) 1.543(2), C(23)−C(24) 1.529(3), Si(1)−C(25) 1.864(2), Si(1)−C(26) 1.870(2), Si(1)−C(27) 1.843(2), Si(1)−Cl(1) 2.084(8); C(25)−Si(1)−Cl(1) 107.2(1), C(26)−Si(1)−Cl(1) 105.4(1), C(27)−Si(1)−Cl(1) 106.4(1).
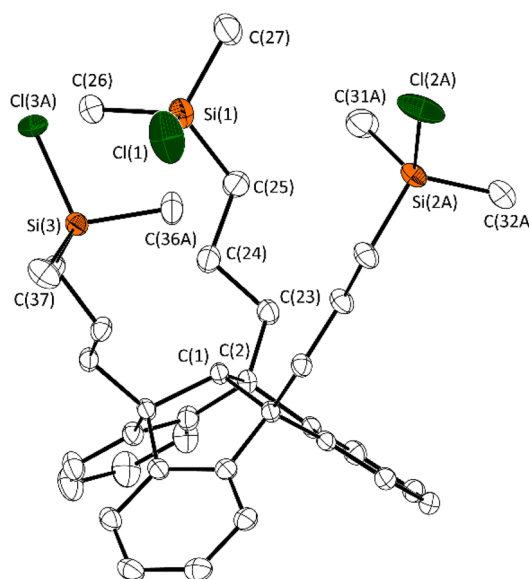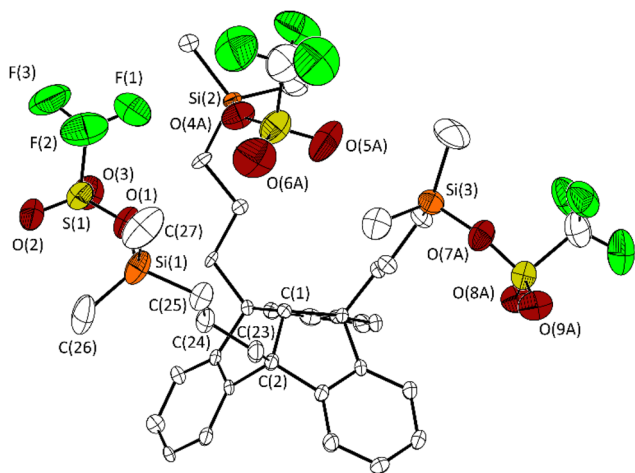
Fig. 2 Molecular structure of **3** in the crystalline state. Displacement ellipsoids are drawn at the 50% probability level. Hydrogen atoms and minor occupied disordered parts are omitted for clarity. Only one of the two crystallographically independent molecules is shown. For further details, see the ESI.† Selected bond lengths [Å] and angles [°]: C(1)−C(2) 1.562(6), C(2)−C(23) 1.541(7), C(23)−C(24) 1.532(7), C(24)−C(25) 1.520(8), Si(1)−C(25) 1.856(5), Si(1)−C(26) 1.844(9), Si(1)−C(27) 1.842(9) Si(1)−O(1) 1.754(5), O(1)−S(1) 1.522(5); C(25)−Si(1)−O(1) 102.0(3), C(26)−Si(1)−O(1) 109.2(3), C(27)−Si(1)−O(1) 105.4(4).

of **1** with dicyclohexylborane, as a colourless solid in quantitative yield (Scheme 2).

The ^{1}H NMR spectrum of **4** shows the characteristic multiplets of the TBTQ backbone, the signals of the propyl groups and of the hydrogen atoms of the cyclohexyl substituents. The ^{11}B NMR chemical shift of 84.3 ppm is in the range of similar compounds.[21]

Regioselective hydroboration of triallyl–TBTQ **1** in *anti*-Markovnikov position with 9-borabicyclo[3.3.1]nonane (9-BBN)
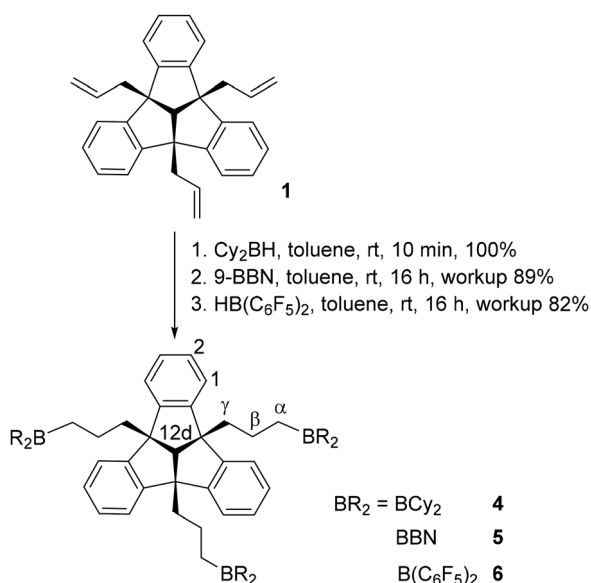
Scheme 2 Syntheses of triboryl–TBTQ compounds **4**, **5** and **6**.

Table 1 Selected ^{1}H NMR chemical shifts [ppm] of compounds **2–6** in C$_6$D$_6$ (500 MHz, 298 K)

Compound	H1	H2	H12d	γ-H	β-H	α-H
2	7.07	7.29	3.78	2.30	1.56	0.81
3	7.10	7.30	3.67	2.24	1.44	0.78
4	7.07	7.33	3.81	2.30	1.59	1.37
5	7.08	7.36	3.97	2.36	1.25	1.54
6	6.96	7.09	3.45	2.18	1.55	2.08

afforded the flexible boron–PLA **5** (Scheme 2). The ^{1}H NMR signal pattern is consistent with that of compound **4** (Table 1). The ^{11}B NMR chemical shift of 89.5 ppm is in the expected region. Since PLAs **4** and **5** are expected to have relatively low Lewis acidity,[22] due to the electron donating alkyl-groups, we introduced stronger electron withdrawing pentafluorophenyl substituents at the boron functions. The hydroboration was carried out in analogy to the syntheses of **4** and **5** with Piers' borane and afforded the bis(pentafluorophenyl)boryl substituted PLA **6** (Scheme 2). The increased Lewis acidity of **6** compared to compounds **2–5** has an effect on the chemical shifts of the signals of **6** in the ^{1}H NMR spectrum (Table 1).

The signals of the TBTQ backbone of **6** are high-field shifted. In contrast, the signal of the hydrogen atom adjacent to the boron atom (α-H) is low-field shifted. The observed ^{11}B NMR signal at 74.3 ppm and the ^{19}F chemical shifts are consistent with those of similar compounds.[7c,10e,g]

Host–guest-experiments

We carried out host–guest experiments by combining the new PLAs **3–6** with (multidentate) Lewis bases to give adducts as shown in Fig. 3. In preliminary tests we used pyridine to demonstrate the reactivity of the PLAs **3–6** towards neutral bases by forming the 1:3 adduct (Fig. 3A). The formation of this type of adduct (**3**·3Py, **4**·3Py, **5**·3Py, **6**·3Py) was observed for each PLA. As expected, all ^{1}H NMR signals of the complexed pyridine are shifted, compared to those of the free pyridine. The adduct formation was further confirmed by ^{19}F NMR
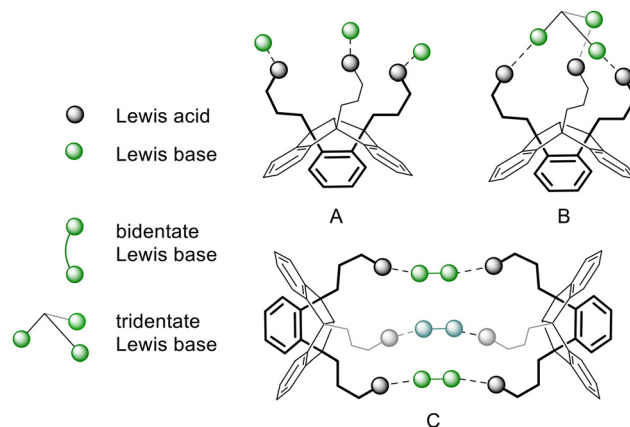

Fig. 3 Structure motifs of a tridentate PLA with monodentate guests (A), tridentate guests (B) and intermolecular linkage *via* bidentate guests (C).

(**3**·3Py and **6**·3Py) and ^{11}B NMR spectroscopy (**4**·3Py, **5**·3Py and **6**·3Py). The ^{19}F resonance of **3**·3Py at −79.1 ppm is high-field shifted relative to that of the free PLA **3** and is in the region of the chemical shift of uncomplexed triflate.[7b] Relative to those of the free PLA, the [11]B resonances of **4**·3Py, **5**·3Py and **6**·3Py are high-field shifted (δ = 8.0 ppm for **4**·3Py, 0.3 ppm for **5**·3Py and 2.9 ppm for **6**·3Py) into the region typically found for tetra-coordinated boron atoms. A single crystal of the adduct **5**·3Py was obtained upon concentration of the reaction mixture and was analysed by X-ray diffraction experiments (Fig. 4).

The molecular structure of **5**·3Py confirms the complexation of three pyridine molecules, resulting in the 1:3 adduct with tetra-coordinated boron atoms. The B–N bond lengths are comparable to similar structures. Due to the flexibility of the propyl spacers, the spatial arrangement of the boron functions is variable, making PLA **5** a suitable host for guest molecules of different sizes.

Compared to the ^{1}H NMR spectra of **4**·3Py and **5**·3Py, the chemical shifts of the resonances of excess and complexed pyridine in **6**·3Py differ significantly, indicating a less dynamic complexation due to the increased Lewis acidity of the boron atoms caused by the electron withdrawing pentafluorophenyl substituents.

Considering the molecular structure of **5**·3Py in Fig. 4, a complexation of tridentate guests is conceivable in the cavity spanned between the boron atoms or in the outer sphere to form adducts as shown in Fig. 3B. We therefore investigated the host–guest interactions of the PLAs **4**–**6** with the tridentate nitrogen base 1,3,5-triazine.

The addition of triazine to a solution of **4** in C_6D_6, did not result in the formation of an adduct, due to the low Lewis acidity of the cyclohexyl-substituted boron atom. In contrast, the ^{1}H NMR spectra indicated complexation of triazine by PLA **5**. We also observed a broadened, high-field shifted [11]B resonance of the adduct at 27.8 ppm. We suggest that this is an averaged signal of complexed and partially free boron functions of PLA **5**, due to a rapid exchange of triazine. Apparently, the spatial orientation of the Lewis base functions does not fit well with that of the Lewis acidic moieties. To gain further insight into the complexation process of **5** and triazine we performed an NMR titration experiment by treating **5** with an increasing concentrations of the guest compound triazine (Fig. 5).

Fig. 5 shows the ^{1}H NMR spectra of the non-complexed PLA **5** and of triazine together with spectra of the PLA **5** (host, H) with an increasing concentration of triazine (guest, G). For a simplified view we only consider the signals of triazine (*), the hydrogen atom in the centre of the TBTQ backbone (*H*12d, #) and of the γ-*H* of the propyl group (•). Addition of small amounts of triazine (0.4 eq.) only results in a slight shift of *H*12d (#) and γ-*H* (•) to higher field. The triazine signal (*) is low-field shifted compared to free triazine, due to the complete complexation of guest molecules. Further addition of guest (1.4 eq.) leads to significantly shifted signals of *H*12d (#) and γ-*H* (•), while the triazine signal (*) experienced no further shift. This is consistent with for the formation of a 1:1 adduct, possibly with dynamic exchange of the guest between the Lewis acidic functions of the host molecule, as suggested by the ^{11}B NMR data. Increasing the guest concentration to 2.4 eq., the resonances of *H*12d (#) and γ-*H* (•) receive a strong high-field shift, while the guest signal (*) approaches the shift of free triazine. This is in agreement with the formation of a 1:3 adduct in which only one of the nitrogen atoms of triazine is complexed. For higher guest concentrations, only minor
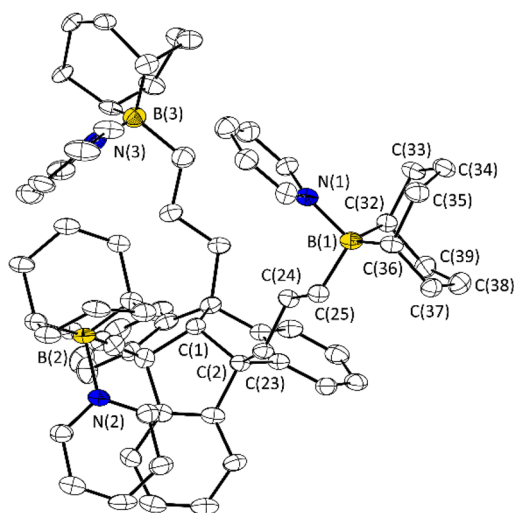

Fig. 4 Molecular structures of **5**·3Py in the crystalline state. Displacement ellipsoids are drawn at the 50% probability level. Hydrogen atoms, solvent benzene molecules and minor occupied dis-ordered parts are omitted for clarity. For further details, see the ESI.† Selected bond lengths [Å] and angles [°]: C(1)−C(2) 1.566(7), C(2)−C(23) 1.531(7), C(23)−C(24) 1.524(6), C(24)−C(25) 1.536(6), B(1)−C(25) 1.626(7), B(1)−C(32) 1.626(7), B(1)−C(36) 1.631(7) B(1)−N(1) 1.646(7); C(25)−B(1)−N(1) 104.2(4), C(25)−B1(1)−C(32) 114.9(4), C(25)−B(1)−C(36) 113.4(4), C(32)−B(1)−C(36) 103.9(4). N(1)−B(1)−C(36) 110.0(4).
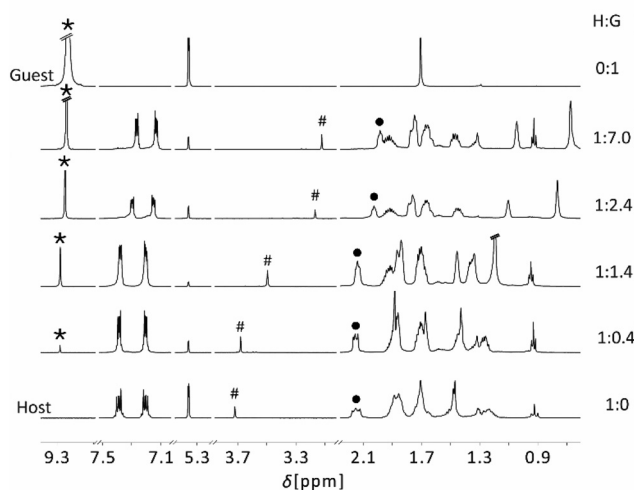

Fig. 5 Series of the ^{1}H NMR spectra of mixtures of host compound **5** with increasing concentration of triazine and free triazine (300 MHz, 298 K).

changes are observed, as all Lewis acidic functions of the host component are complexed by guest molecules.

We observed a similar complexation behaviour of triazine with PLA **6**. As expected, the triazine signal of **6**·triazine is further low-field shifted, compared to the signal of **5**·triazine, due to the stronger Lewis acidity of **6**. Also, the averaged signal of complexed and free Lewis acidic functions of **6** with a chemical shift of 40.4 ppm in the ^{11}B NMR spectrum is consistent with the host–guest experiment of **5** and triazine.

To elucidate the effect of the Lewis basic function on the complexation with boron PLAs, we also carried out an exemplary host–guest experiment with PLA **5** and PMe$_3$ and further experiments with the tridentate phosphorus Lewis base tris(dimethylphosphinomethyl)phenylsilane (TrisPhos, (Me$_2$PCH$_2$)$_3$SiPh). As expected, the conversion of PLA **5** with PMe$_3$ resulted in the formation of the corresponding 1 : 3 adduct **5**·PMe$_3$. In addition to the TBTQ signals, the doublet of the PMe$_3$ is also shifted in the ^{1}H NMR spectrum. The chemical shifts of −4.1 ppm in the ^{11}B NMR and of 15.6 ppm in the ^{31}P{^{1}H} NMR spectrum are indicative of the formation of the adduct **5**·PMe$_3$. The addition of one equivalent of TrisPhos to a solution of **5** in CDCl$_3$ resulted in the selective formation of the 1 : 1 adduct **5**·TrisPhos, according to the NMR spectroscopy (Fig. 6).

We observed a shift for all signals of PLA **5** and TrisPhos. Compared to **5**·triazine, the observed signals of **5**·TrisPhos are narrow, especially those of the guest, indicating a much slower or no exchange dynamics and therefore a comparatively stable 1 : 1 adduct. Apparently, the higher flexibility of TrisPhos compared to triazine allows the adjustment of the Lewis base functions to the spatial orientation of the Lewis acidic moieties. The chemical shifts of 9.1 ppm in the ^{11}B and −27.2 ppm in the ^{31}P{^{1}H} NMR spectrum are consistent with an adduct formation.

In contrast, there is a more dynamic complexation process between TrisPhos and **4** in CDCl$_3$. The ^{1}H, ^{31}P{^{1}H} and ^{11}B NMR spectra show strongly broadened signals, due to the lower Lewis acidity of the cyclohexyl-substituted boron function and the associated small equilibrium constant of the adduct formation.

Although, the addition of TrisPhos to a solution of **6** in CDCl$_3$ resulted in a shift of the ^{1}H NMR signals, the many signals of host and guest indicate the formation of different adduct species or oligomers. Due to the high Lewis acidity of **6**, the reversibility of this adduct formation is limited.

In order to elucidate the data obtained from the NMR titration of **5** with triazine and the host–guest experiment of **5** with TrisPhos, we have further studied the adduct formation in more detail by means of ^{1}H DOSY NMR experiments. According to the Stokes–Einstein (SE) equation, the experimentally accessible diffusion coefficient D is inversely proportional to the hydrodynamic radius (r_H) of the diffusing particle.[24] A comparison of D of PLA **5** and the corresponding Lewis base with those of the host–guest adducts should therefore provide information about the aggregate formed in solution. The van der Waals volumes (V_{vdW}) of host, guest and adduct give a first indication about the dimensions of the hydrodynamic volumes (V_H). Table 2 shows the van der Waals volumes (V_{vdW}) calculated using the method reported by Abraham *et al.*,[25] the measured and corrected diffusion coefficients, the hydrodynamic radii (r_H) and volumes (V_H) calculated using the Stokes–Einstein equation.

The diffusion NMR experiment of PLA **5** and one equivalent triazine reveals a different composition of the aggregate than we initially assumed from the ^{1}H NMR spectrum. The hydrodynamic volume V_H determined from the host component **5** in the adduct **5**·triazine, results in a larger value (1335 Å^3) than the sum of those of the single components: V_H of host **5** is 967 Å^3 and that of free triazine is 138 Å^3. The V_H of the guest part (620 Å^3) in **5**·triazine indicates a fast exchange of triazine molecules and a small equilibrium constant, due to the presence of free guest molecules. The DOSY experiment sees only an average in time of the bound and free triazine molecules and their V_H is therefore between that of the free triazine and that measured for the component **5** in the adduct. This dynamic process is in agreement with the slightly broadened signals in the ^{1}H and ^{11}B NMR spectra.

In contrast, the ^{1}H DOSY NMR experiment of **5** with TrisPhos is in accordance with the NMR data we discussed
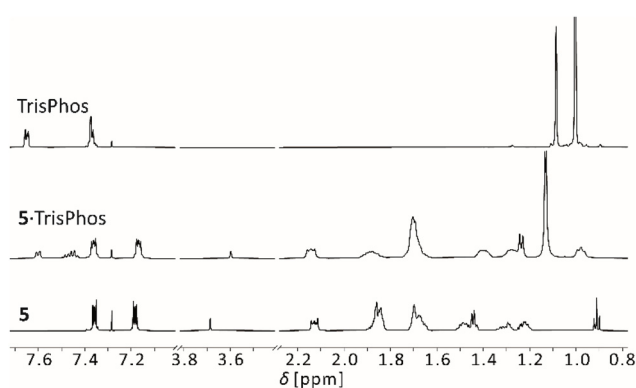

Fig. 6 Sections of the ^{1}H NMR spectra of TrisPhos, PLA **5** (600 MHz, 293 K) and the adduct **5**·TrisPhos (500 MHz, 298 K) in CDCl$_3$.

Table 2 van der Waals volumes (V_{vdW}) calculated by a method of Abraham *et al.*,[25] diffusion coefficients (D), hydrodynamic radii (r_H) and hydrodynamic volumes (V_H) of compound **5**, triazine, tris(dimethylphosphinomethyl)phenylsilane (TrisPhos) and of the adducts **5**·triazine and **5**·TrisPhos. For diffusion NMR details see the ESI†

Compound	V_{vdW} [Å^3]	V_{XRD} [Å^3]	D [10^{-10} m^2 s^{-1}] Host/guest	r_H [Å] Host/guest	V_H [Å^3] Host/guest
5	945	—	6.17/—	6.14/—	967/—
Triazine	115	98 [26]	18.7/—	2.03^a/—	138^a/—
TrisPhos	390	—	9.14/—	4.95^a/—	508^a/—
5·triazine	1060	—	5.54/7.16	6.83/5.29	1335/620
5·TrisPhos	1335	—	5.25/7.16	7.22/7.04	1574/1463

^{a} Calculated by a modified formula, that is suitable for small molecules. For further details see the ESI.†

above and confirms the formation of a 1 : 1 adduct. The determined hydrodynamic volumes of the adduct **5**·TrisPhos (1574 Å^3 (host part), 1463 Å^3 (guest part)) are approximately

the sum of the hydrodynamic volume of the host **5** (967 Å^3) and of TrisPhos (508 Å^3).

Further host–guest experiments were carried out with PLA **3** (H) and the bidentate base 3,3′-bipyridine (G), to obtain a 2 : 3 adduct ($[H_2G_3]^{6+}$) with a cage-like structure as shown in Fig. 3C. The aggregation process was followed by ^{1}H DOSY NMR titration experiments: we gradually added 3,3′-bipyridine to a solution of **3** in acetonitrile; in addition, the diffusion coefficient of the triflate component was followed by ^{19}F DOSY NMR. From these D values, we calculated the hydrodynamic radii (r_H) for host and guest (^{1}H) and triflate (^{19}F) and calculated their hydrodynamic volumes (V_H). Since acetonitrile has already been shown to be a suitable solvent for ionic com-

Table 3 Hydrodynamic radii (r_H) and volumes (V_H) of compound **3** and the reference compound [**3**·3*p*PhPy] determined of the diffusion coefficients from the diffusion measurements

Compound	Obs. nucl.	r_H [Å]	V_H [Å^3]	V_{XRD}
3	^{1}H	5.13	1331	1244
	^{19}F	6.31	567	
3·3*p*PhPy	^{1}H	7.43	1721	—
	^{19}F	3.30	150	
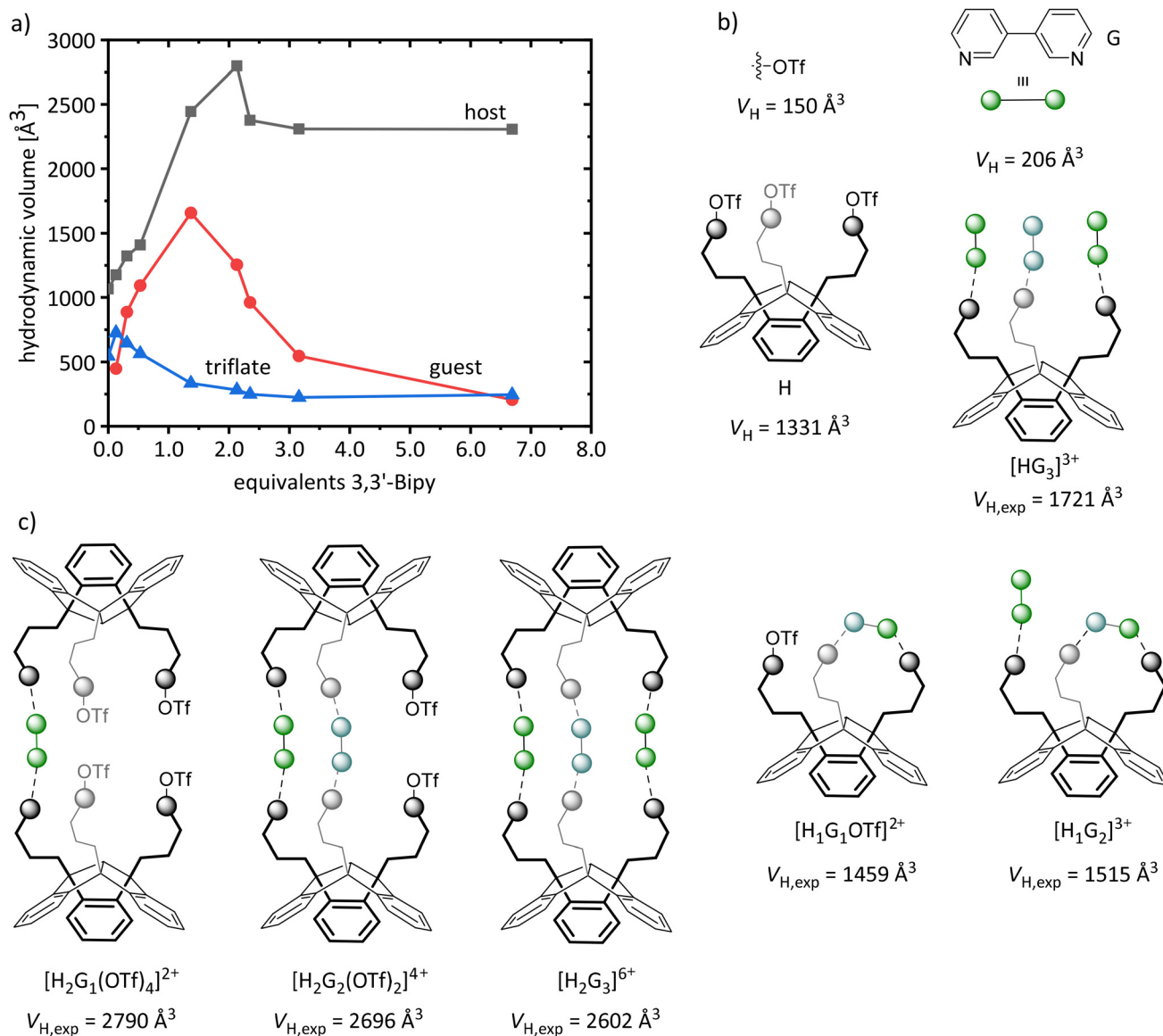
Fig. 7 (a) Calculated hydrodynamic volumes (V_H) of host (■, **3**), guest (●, 3,3′-bipyridine) and triflate (▲) component, derived from the ^{1}H and ^{19}F DOSY NMR experiments as a function of the equivalents of the guest (3,3′-Bipy); (b) determined hydrodynamic volumes (V_H) of host, guest triflate and the HG$_3$$^{3+}$ adduct derived from the DOSY measurements of the host **3** and the reference compound **3**·3*p*PhPy; (c) potentially formed adducts and their expected hydrodynamic volume ($V_{H,exp}$) in the DOSY titration experiment of **3** and 3,3′-bipyridine.

pounds formed during the adduct formation,[7b] it was also used in this experiment.

For a more precise interpretation of the diffusion data, additional measurements of the free PLA **3** were performed, as well as of the adduct of **3** with *p*-phenylpyridine (**3**·3*p*PhPy), as highly similar reference compound for a monodentate acting 3,3′-bipyridine; in this way we intended to simulate the saturation of the Lewis acidic functions by formation of a $[HG_3]^{3+}$ adduct as shown in Fig. 3A and to obtain its corresponding hydrodynamic volume (1721 Å^3, Table 3). It is noteworthy, that we observed a deviation of the hydrodynamic volume of **3** (V_H = 1331 Å^3) determined by ^{1}H DOSY NMR from that determined using ^{19}F DOSY NMR (for the triflate substituents of **3**, V_H = 567 Å^3). Consistently, VT NMR experiments of **3** also show deviations for the triflate component: with increasing temperature, we determined a decrease in the hydrodynamic volume of **3**, indicating a partial dissociation of the triflate substituents from the core of **3**.

Fig. 7 shows the calculated hydrodynamic volumes (V_H) of host, guest and triflate for the corresponding equivalents of 3,3′-bipyridine, as well as the hydrodynamic volumes of the individual components, derived from the DOSY measurements of the host **3** and the reference compound **3**·3*p*PhPy. In addition it shows the potentially formed adducts and their corresponding expected hydrodynamic volumes ($V_{H,exp}$) calculated from the determined values of the reference compound. Without guest component, we observe a deviation of the hydrodynamic volumes (V_H) of host and triflate in the diffusion NMR measurement of the free PLA **3**, as mentioned above.

As expected, the hydrodynamic volume (V_H) of triflate decreases with increasing guest concentration. Remarkably, the V_H of host and guest already differ at low guest concentrations, indicating a small equilibrium constant and the presence of free guest molecules. Addition of only 1.3 eq. of the guest leads to a rapid increase of the V_H of the host (2512 Å^3), which corresponds to a $[H_2G_x]^{(x+1)+}$ adduct. Further addition of guest component (2.13 eq.) leads to a $V_{H,max.}$ of 2798 Å^3. Considering a V_H of 1721 Å^3 for $[HG_3]^{3+}$, 1331 Å^3 for H and 150 Å^3 for triflate (Table 3), we expect a $V_{H,max.}$ of approximately 2602 Å^3 for $[H_2G_3]^{6+}$ (Fig. 7). The deviation is most possibly a result of a mixture of different $[H_2G_x]^{(x+1)+}$ aggregates and partially non-complexed host and guest molecules resulting from the fast exchange. Even the intramolecular complexation of 3,3′-bipyridine by two Lewis acidic sites of one host molecule ($[H_1G_1OTf]^{2+}$, $[H_1G_2]^{3+}$; Fig. 7) must be taken into consideration here.

The addition of 6.9 eq. of the guest leads to a final hydrodynamic volume of 2307 Å^3 (H) and a continuous decrease of the V_H of the guest (206 Å^3) as increasingly non-complexed guest compound becomes the predominant component in solution. Remarkably, even for high guest concentrations the aggregates of the composition $[H_2G_x]^{(x+1)+}$ are present in solution. The formation of larger oligomers or chain structures can be ruled out as the aggregates formed showed a high solubility throughout the entire titration experiment.

Conclusions

Various flexible poly-Lewis acids based on the tribenzotriquinacene (TBTQ) scaffold have been synthesised in hydrometallation reactions of 4b,8b,12b-triallyltribenzotriquinacene with hydrochlorosilanes and hydroboranes. The Lewis acidity of the introduced silyl functions was increased by substituting their chloro substituents with weaker coordinating triflate groups. Host–guest experiments with pyridine demonstrated the reactivity of the new PLAs. The complexation behaviour of the boron-functionalised PLAs was exemplarily studied for the host–guest interaction of the boryl-substituted PLA **5** with triazine and tris(dimethylphosphinomethyl)phenylsilane (TrisPhos) in ^{1}H DOSY NMR experiments. This proved to be a suitable method for the analysis of host–guest aggregates, as it revealed a contrasting composition of the formed adduct to that suggested by the ^{1}H NMR spectra. It also emphasises the high dynamics involved in the aggregation processes. The complexation of TrisPhos with PLA **5** proved to be less dynamic and the determined hydrodynamic volume corresponds to the formation of a 1 : 1 adduct, which is consistent with the ^{1}H NMR data. The complexation of the boron-functionalised PLAs **4–6** also showed the influence of the Lewis acidity on the constitution of the adducts. Further diffusion experiments were carried out with the tris(triflatosilyl)-substituted PLA **3** and 3,3′-bipyridine. The titration experiment showed again the complexity of host–guest reactions in solution. The determined hydrodynamic volume of the host component indicates a linkage of two host molecules by up to three guests, while the formation of larger oligomers can be ruled out. The dynamics of the aggregation process do not allow more detailed conclusions to be drawn about the number of guest molecules bound. Overall, the results show that we often observe a counterintuitive behaviour of the aggregations processes and not only the simplest possible or highest symmetry adducts are formed.
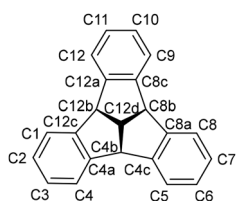
Experimental section

General remarks

4b,8b,12b-Tribromotribenzotriquinacene and 4b,8b,12b-triallyltribenzotriquinacene (**1**) were synthesised according to literature protocols.[20,23] All reagents for host–guest experiments were dried under vacuum or freshly distilled before use. All reactions involving oxidation- or hydrolysis-sensitive substances were carried out using standard Schlenk techniques or in glove boxes under inert nitrogen or argon atmospheres. Solvents were freshly dried and degassed (benzene, toluene and *n*-hexane, dried over Na/K alloy; *n*-pentane and Et$_2$O, dried over LiAlH$_4$; dichloromethane over calcium hydride and THF dried over potassium). NMR spectra were recorded on a *Bruker Avance III 300*, *Bruker Avance III 500 HD* and *Bruker Avance NEO 600* instrument at 298 K and 293 K (DOSY) respectively. Chemical shifts (δ) were measured in ppm with respect to the solvents (C$_6$D$_6$: ^{1}H NMR δ = 7.16 ppm, ^{13}C NMR δ =

128.06 ppm; CDCl$_3$: ^{1}H NMR δ = 7.26 ppm, ^{13}C NMR δ = 77.16 ppm; CD$_2$Cl$_2$: ^{1}H NMR δ = 5.32 ppm, ^{13}C NMR δ = 53.84 ppm, CD$_3$CN: ^{1}H NMR δ = 1.94 ppm, ^{13}C NMR δ = 1.32 ppm, 118.26 ppm) or referenced externally (^{11}B: BF$_3$·Et$_2$O, ^{19}F: CFCl$_3$; ^{29}Si: SiMe$_4$; ^{31}P: 85% H$_3$PO$_4$,). Elemental analyses were performed using a *HEKAtech EURO EA* instrument. Assignments of the NMR-signals are based on the IUPAC guidelines and are shown in Scheme 3.

4b,8b,12b-Tris(3-(chloro(dimethyl)silyl)propyl)-tribenzotriquinacene (2, IUPAC: 4b,8b,12b-tris(3-(chloro(dimethyl)silyl)propyl)-4b,8b,12b,12d-tetrahydrodibenzo[2,3:4,5]pentaleno[1,6-*ab*]indene). 4b,8b,12b-Triallyltribenzotriquinacene (**1**, 500 mg, 1.25 mmol) was dissolved in chlorodimethylsilane (10 mL). Two drops of a solution of platinum(0)-1,3-divinyl-1,1,3,3-tetramethylsiloxane (2% Pt solv. in xylene) were added and the solution was heated at 40 °C for 72 h. All volatile components were removed under reduced pressure and the crude product was washed with *n*-hexane (2 mL) to yield **2** as a colourless solid (0.72 g, 1.1 mmol, 84%). Single crystals for X-ray diffraction were obtained by cooling a saturated solution of **2** in *n*-hexane at −30 °C. ^{1}H NMR (500 MHz, C$_6$D$_6$): δ = 7.29 (m, 6H, *H*2/*H*3/*H*6/*H*7/*H*10/*H*11) 7.07 (m, 6H *H*1/*H*4/*H*5/*H*8/*H*9/*H*12), 3.78 (s, 1H, *H*12d), 2.30 (m, 6H, C*H*$_2$CH$_2$CH$_2$Si), 1.56 (m, 6H, CH$_2$C*H*$_2$CH$_2$Si), 0.81 (m, 6H, CH$_2$CH$_2$C*H*$_2$Si), 0.20 (s, 18H, Si(C*H*$_3$)$_2$Cl) ppm. ^{13}C{^{1}H} NMR (126 MHz, C$_6$D$_6$) δ = 148.8 (*C*4a/*C*4c/*C*8a/*C*8c/*C*12a/*C*12c), 128.0 (*C*2/*C*3/*C*6/*C*7/*C*10/*C*11), 123.0 (*C*1/*C*4/*C*5/*C*8/*C*9/*C*12), 67.9 (*C*12d), 64.3 (*C*4b/*C*8b/*C*12b), 45.3 (*C*H$_2$CH$_2$CH$_2$Si), 20.1 (CH$_2$*C*H$_2$CH$_2$Si), 19.5 (CH$_2$CH$_2$*C*H$_2$Si), 1.80 (Si(*C*H$_3$)$_2$Cl) ppm. ^{29}Si{^{1}H} NMR (60 MHz, C$_6$D$_6$) δ = 31.2 ppm. Elemental analysis calcd (%) for C$_{37}$H$_{49}$Cl$_3$Si$_3$ (684.40): C 64.93 H 7.22; found C 63.67 H 7.53.

4b,8b,12b-Tris(3-(trifluoromethylsulfonyl(dimethyl)silyl)propyl)-tribenzotriquinacene (3, IUPAC: 4b,8b,12b-tris(3-(tri-fluoromethylsulfonyl(dimethyl)silyl)propyl)-4b,8b,12b,12d-tetrahydrodibenzo[2,3:4,5]pentaleno[1,6-*ab*]indene). Silver triflate (506 mg, 1.97 mmol) was suspended in dichloromethane (2 mL) and 4b,8b,12b-tris(3-(chlorodimethylsilyl)propyl)-tribenzotriquinacene (**2**, 392 mg, 0.57 mmol) dissolved in dichloromethane (5 mL) was added. The suspension was stirred for 3 d under absence of light at room temperature and was then filtered. After removal of the solvent under reduced pressure a brown resin was afforded which was extracted with *n*-hexane. After concentration of the hexane solution and cooling at −30 °C, colourless crystals were obtained. The supernatant solution was removed with a syringe and the crystalline residue was dried in vacuum to yield **3** as a colourless

solid (490 mg, 0.48 mmol, 84%). Single crystals for X-ray diffraction were obtained by cooling a saturated solution of **3** in *n*-hexane at −30 °C. ^{1}H-NMR (500 MHz, CD$_3$CN) δ = 7.42 (m, 6H, *H*2/*H*3/*H*6/*H*7/*H*10/*H*11). 7.19 (m, 6H, *H*1/*H*4/*H*5/*H*8/*H*9/*H*12), 3.49 (s, 1H, *H*12d), 2.16 (m, 6H, C*H*$_2$CH$_2$CH$_2$Si), 1.31 (m, 6H, CH$_2$C*H*$_2$CH$_2$Si), 0.96 (t, $^3J_{H,H}$ = 8.2 Hz, 6H, CH$_2$CH$_2$C*H*$_2$Si), 0.41 (s, 18H, Si(C*H*$_3$)$_2$OTf) ppm. ^{13}C{^{1}H}-NMR (126 MHz, CD$_3$CN) δ = 149.2 (*C*4a/*C*4c/*C*8a/*C*8c/*C*12a/*C*12c), 128.7 (*C*2/*C*3/*C*6/*C*7/*C*10/*C*11), 124.0 (*C*1/*C*4/*C*5/*C*8/*C*9/*C*12), 119.5 (q, $^1J_{F,C}$ = 317 Hz, *C*F$_3$) 67.9 (*C*12d), 64.8 (*C*4b/*C*8b/*C*12b), 45.2 (*C*H$_2$CHCH$_2$Si), 19.6 (CH$_2$*C*H$_2$CH$_2$Si), 17.2 (CH$_2$CH$_2$*C*H$_2$Si), −2.2 (Si(*C*H$_3$)$_2$OTf) ppm. ^{19}F-NMR (471 MHz, CD$_3$CN) δ = −78.5 ppm. ^{29}Si{^{1}H}-NMR (60 MHz, CD$_3$CN) δ = 45.6 ppm.

^{1}H-NMR (300 MHz, C$_6$D$_6$) δ = 7.30 (m, 6H, *H*2/*H*3/*H*6/*H*7/*H*10/*H*11). 7.10 (m, 6H, *H*1/*H*4/*H*5/*H*8/*H*9/*H*12), 3.67 (s, 1H, *H*12d), 2.24 (m, 6H, C*H*$_2$CH$_2$CH$_2$Si), 1.44 (m, 6H, CH$_2$C*H*$_2$CH$_2$), 0.78 (t, $^3J_{H,H}$ = 7.9 Hz, 6H, CH$_2$CH$_2$C*H*$_2$Si), 0.08 (s, 18H, Si(C*H*$_3$)$_2$OTf) ppm. ^{13}C{^{1}H}-NMR (75.5 MHz, C$_6$D$_6$) δ = 148.6 (*C*4a/*C*4c/*C*8a/*C*8c/*C*12a/*C*12c), 128.1 (*C*2/*C*3/*C*6/*C*7/*C*10/*C*11), 123.2 (*C*1/*C*4/*C*5/*C*8/*C*9/*C*12), 67.8 (*C*12d), 64.1 (*C*4b/*C*8b/*C*12b), 45.2 (*C*H$_2$CH$_2$CH$_2$Si), 19.1 (CH$_2$*C*H$_2$CH$_2$Si), 16.7 (CH$_2$CH$_2$*C*H$_2$Si), 0.8 (Si(*C*H$_3$)$_2$OTf) −1.8 (Si(*C*H$_3$)$_2$) ppm (resonances for *C*F$_3$ were not observed). ^{19}F-NMR (282 MHz, C$_6$D$_6$) δ = −77.4 ppm. ^{29}Si{^{1}H}-NMR (99 MHz, C$_6$D$_6$) δ = 43.9 ppm. Elemental analysis calcd (%) for C$_{40}$H$_{49}$F$_9$O$_9$S$_3$Si$_3$ (1025.24): C 46.86 3 H 4.82 S 9.38; found C 47.58 H 4.75 S 8.69.

4b,8b,12b-Tris(3-(dicyclohexylboryl)propyl)-tribenzotriquinacene (4, IUPAC: 4b,8b,12b-tris(3-(dicyclohexylboryl)propyl)-4b,8b,12b,12d-tetrahydrodibenzo[2,3:4,5]pentaleno[1,6-*ab*]indene). Dicyclohexylborane (138 mg, 0.77 mmol) was added to a solution of 4b,8b,12b-triallyltribenzotriquinacene (**1**, 100 mg, 0.25 mmol) in benzene (1 mL) and stirred for 10 min at room temperature. All volatiles were removed under reduced pressure to afford 4b,8b,12b-tris(dicyclohexylborylpropyl)-tribenzotriquinacene (**4**, 234 mg, 0.25 mmol) as a colourless solid. ^{1}H-NMR (500 MHz, C$_6$D$_6$) δ = 7.33 (m, 6H, *H*2/*H*3/*H*6/*H*7/*H*10/*H*11) 7.07 (m, 6H, *H*1/*H*4/*H*5/*H*8/*H*9/*H*12), 3.81 (s, 1H, *H*12d), 2.30 (m, 6H, C*H*$_2$CH$_2$CH$_2$B), 1.84–1.13 (m, 33H, overlapping Cy–*H*) 1.59 (m, 6H CH$_2$C*H*$_2$CH$_2$B), 1.37 (t, $^3J_{H,H}$ = 7.8 Hz, 6H, CH$_2$CH$_2$C*H*$_2$B). ^{13}C{^{1}H}-NMR (126 MHz, C$_6$D$_6$) δ = 149.1 (*C*4a/*C*4c/*C*8a/*C*8c/*C*12a/*C*12c), 128.0 (*C*2/*C*3/*C*6/*C*7/*C*10/*C*11), 123.4 (*C*1/*C*4/*C*5/*C*8/*C*9/*C*12), 68.2 (*C*12d), 64.4 (*C*4b/*C*8b/*C*12b), 46.0 (*C*H$_2$CH$_2$CH$_2$B), 36.1 (Cy–*C*1), 28.1 (Cy–*C*3, Cy–*C*5) 27.6 (Cy–*C*2, Cy–*C*6), 26.9 (CH$_2$*C*H$_2$CH$_2$B), 26.1 (Cy–*C*4), 21.1 (CH$_2$CH$_2$*C*H$_2$B). ^{11}B-NMR (160 MHz, C$_6$D$_6$) δ = 84.3. Elemental analysis calcd (%) for C$_{67}$H$_{97}$B$_3$ (934.94): C 86.07 H 10.96; found C 84.66 H 11.21.

4b,8b,12b-Tris(3-(9-borabicyclo[3.3.1]nonanyl)propyl)-tribenzotriquinacene (5, IUPAC: 4b,8b,12b-tris(3-(9-borabicyclo[3.3.1]nonanyl)propyl)-4b,8b,12b,12d-tetrahydrodibenzo[2,3:4,5]pentaleno[1,6-*ab*]indene). 4b,8b,12b-Triallyltribenzotriquinacene (**1**, 310 mg, 0.77 mmol) was dissolved in toluene (5 mL) and 9-BBN solution (0.5 M in THF, 4.7 mL, 2.4 mmol) was added. The solution was stirred at room temperature for 16 h. Removal of the solvents under reduced pressure obtained a crude product which was dissolved in a small amount of

Scheme 3 Numbering scheme of the tribenzotriquinacene skeleton for NMR assignments.

n-hexane and precipitated at −30 °C. The supernatant solution was removed with a syringe and the crystalline residue was dried in vacuum to yield **5** (525 mg, 0.69 mmol, 89%) as a colourless solid. ^{1}H-NMR (500 MHz, C$_6$D$_6$) δ = 7.36 (m, 6H, *H*2/ *H*3/*H*6/*H*7/*H*10/*H*11), 7.08 (m, 6H, *H*1/*H*4/*H*5/*H*8/*H*9/*H*12), 3.97 (s, 1H, *H*12d), 2.36 (m, 6H, CH$_2$CH$_2$CH$_2$B), 2.51–2.08 (m, 48H, overlapping BBN–*H*, CH$_2$C*H*$_2$CH$_2$B), 1.78 (t, $^3J_{\text{H,H}}$ = 7.1 Hz, 6H, CH$_2$CH$_2$C*H*$_2$B). ^{13}C{^{1}H}-NMR (126 MHz, C$_6$D$_6$) δ = 149.2 (*C*4a/ *C*4c/*C*8a/*C*8c/*C*12a/*C*12c), 128.4 (*C*2/*C*3/*C*6/*C*7/*C*10/*C*11), 123.4 (*C*1/*C*4/*C*5/*C*8/*C*9/*C*12), 68.1 (*C*12d), 64.5 (*C*4b/*C*8b/*C*12b), 45.7 (*C*H$_2$CH$_2$CH$_2$B), 33.2–22.7 (overlapping BBN–*C*), 21.6 (CH$_2$*C*H$_2$CH$_2$B), 14.4 (CH$_2$CH$_2$*C*H$_2$B). ^{11}B-NMR (160 MHz, C$_6$D$_6$) δ = 89.5. Elemental analysis calcd (%) for C$_{55}$H$_{73}$B$_3$ (766.62): C 86.17 H 9.60; found C 83.09 H 9.60.

4b,8b,12b-Tris(3-(bis(pentafluorophenyl)boranyl)propyl)-tribenzotriquinacene (6, IUPAC: 4b,8b,12b-tris(3-(bis(pentafluorophenyl)boranyl)propyl)-4b,8b,12b,12d-tetrahydrodibenzo[2,3:4,5]pentaleno[1,6-*ab*]indene). 4b,8b,12b-Triallyltribenzotriquinacene (**1**, 100 mg, 0.25 mmol) and bis(pentafluorophenyl) borane (266 mg, 0.77 mmol) were dissolved in toluene (2 mL). The solution was stirred for 1.5 h at room temperature until the solvent was removed under reduced pressure. The residue was dissolved in *n*-hexane and precipitated at −30 °C. The supernatant solution was removed with a syringe and the solid residue was dried *in vacuo* 4b,8b,12b-tris(3-(bis(pentafluorophenyl)boryl)propyl)tribenzotriquinacene (**6**, 294 mg, 0.21 mmol, 82%) was obtained as a colourless solid. ^{1}H-NMR (500 MHz, CD$_2$Cl$_2$) δ = 7.15 (m, 6H, *H*2/*H*3/*H*6/*H*7/*H*10/*H*11) 7.09 (m, 6H, *H*1/*H*4/*H*5/*H*8/*H*9/*H*12), 3.26 (s, 1H, *H*12d), 2.10 (m, 6H, CH$_2$C*H*$_2$CH$_2$B), 2.03 (m, 6H, C*H*$_2$CH$_2$CH$_2$B), 1.38 (m, 6H, CH$_2$CH$_2$C*H*$_2$) ppm. ^{13}C{^{1}H}-NMR (126 MHz, CD$_2$Cl$_2$) δ = 148.3 (*C*4a/*C*4c/*C*8a/*C*8c/*C*12a/*C*12c), 147.3 (dm, $^1J_{\text{F,C}}$ = 253 Hz, *m*-*C*$^{\text{PhF}}$), 143.9 (dm, $^1J_{\text{F,C}}$ = 258 Hz, *o*-*C*$^{\text{PhF}}$), 137.9 (dm, $^1J_{\text{F,C}}$ = 257 Hz *p*-*C*$^{\text{PhF}}$), 128.0 (*C*2/*C*3/*C*6/*C*7/*C*10/*C*11), 123.1 (*C*1/*C*4/*C*5/*C*8/*C*9/*C*12), 67.9 (*C*12d), 64.1 (*C*4b/*C*8b/*C*12b), 44.8 (*C*H$_2$CH$_2$CH$_2$B), 32.8 (CH$_2$*C*H$_2$CH$_2$B), 21.3 (CH$_2$CH$_2$*C*H$_2$B). ^{11}B-NMR (160 MHz, CD$_2$Cl$_2$) δ = 74.3 (s, br) ppm. ^{19}F-NMR (471 MHz, CD$_2$Cl$_2$) δ = −130.3 (m, 4F, *o*-*F*$^{\text{PhF}}$), −148.4 (m, 2F, *p*-*F*$^{\text{PhF}}$), −161.7 (m, 4F, *m*-*F*$^{\text{PhF}}$) ppm. Elemental analysis calcd (%) for C$_{67}$H$_{31}$B$_3$F$_{30}$ (1438.37): C 55.95 H 2.17; found C 56.22 H 2.28.

General procedure for the host–guest experiments

10–15 mg of the host compound was dissolved in a NMR tube fitted with a PTFE tap in C$_6$D$_6$, CD$_2$Cl$_2$, CDCl$_3$ or CD$_3$CN and the corresponding guest compound was added. The host–guest mixture was then analysed by ^{1}H NMR (**3–7**), ^{11}B NMR (**4–6**) and ^{19}F NMR spectroscopy (**2** and **6**).

3·3Py. ^{1}H-NMR (500 MHz, CD$_3$CN) δ = 8.69 (m, 6H, *o*-Py–*H*), 8.54 (m, 3H, *p*-Py–*H*), 8.01 (m, 6H, *m*-Py–*H*), 7.34 (m, 6H, *H*2/ *H*3/*H*6/*H*7/*H*10/*H*11). 7.16 (m, 6H, *H*1/*H*4/*H*5/*H*8/*H*9/*H*12), 3.34 (s, 1H, *H*12d), 1.98 (m, 6H, C*H*$_2$CH$_2$CH$_2$Si), 1.17 (m, 6H, CH$_2$C*H*$_2$CH$_2$Si), 1.13 (m, 6H, CH$_2$CH$_2$C*H*$_2$Si), 0.61 (s, 18H, Si (C*H*$_3$)$_2$OTf) ppm. ^{19}F-NMR (471 MHz, CD$_3$CN) δ = −79.1 ppm.

4·3Py. ^{1}H-NMR (500 MHz, C$_6$D$_6$) δ = 8.31 (d, $^3J_{\text{H,H}}$ = 5.4 Hz, 6H, *o*-Py–*H*), 7.35 (m, 6H, *H*2/*H*3/*H*6/*H*7/*H*10/*H*11), 7.06 (m, 6H, *H*1/*H*4/*H*5/*H*8/*H*9/*H*12), 6.86 (t, $^3J_{\text{H,H}}$ = 7.7 Hz, 3H, *p*-Py–*H*), 6.59

(t, $^3J_{\text{H,H}}$ = 6.6 Hz, 6H, *m*-Py–*H*), 3.86 (s, 1H, *H*12d), 2.37 (m, 6H, C*H*$_2$CH$_2$CH$_2$B), 2.08–0.82 (m, 45H, CH$_2$C*H*$_2$CH$_2$B, overlapping Cy–*H*) ppm. ^{11}B NMR (160 MHz, C$_6$D$_6$) δ = 8.0 (s, br) ppm.

5·3Py. ^{1}H-NMR (300 MHz, CDCl$_3$) δ = 8.36 (m, *o*-Py–*H*), 7.76 (t, $^3J_{\text{H,H}}$ = 7.6 Hz, 3H, *p*-Py–*H*), 7.37 (t, $^3J_{\text{H,H}}$ = 6.6 Hz, 6H, *m*-Py–*H*), 7.04 (m, 6H, *H*2/*H*3/*H*6/*H*7/*H*10/*H*11) 6.93 (m, 6H, *H*1/*H*4/*H*5/*H*8/ *H*9/*H*12), 2.97 (s, 1H, *H*12d), 2.03–0.24 (m, 60H, CH$_2$CH$_2$CH$_2$B, overlapping BBN–*H*) ppm. ^{11}B NMR (160 MHz, CDCl$_3$) δ = 9.2 (s, br) ppm. ^{11}B NMR (96 MHz, CDCl$_3$) δ = 0.3 (s, br) ppm.

6·3Py. ^{1}H-NMR (300 MHz, CD$_2$Cl$_2$) δ = 8.56 (d, $^3J_{\text{H,H}}$ = 6.1 Hz, 6H, *o*-Py–*H*), 8.07 (t, $^3J_{\text{H,H}}$ = 7.7 Hz, 3H, *p*-Py–*H*), 7.60 (t, $^3J_{\text{H,H}}$ = 6.8 Hz, 6H, *m*-Py–*H*), 7.14 (m, 6H, *H*2/*H*3/*H*6/*H*7/*H*10/*H*11) 7.03 (m, 6H, *H*1/*H*4/*H*5/*H*8/*H*9/*H*12), 2.96 (s, 1H, *H*12d), 1.77 (t, $^3J_{\text{H,H}}$ = 8.1 Hz, 6H, CH$_2$CH$_2$C*H*$_2$B), 1.17 (m, 6H, CH$_2$C*H*$_2$CH$_2$B), 0.57 (m, 6H, C*H*$_2$CH$_2$CH$_2$B), ppm. ^{11}B NMR (96 MHz, CD$_2$Cl$_2$) δ = 2.9 (s, br) ppm. ^{19}F-NMR (282 MHz, CD$_2$Cl$_2$) δ = −132.5 (m, 4F, *o*-*F*$^{\text{PhF}}$), −159.4 (m, 2F, *p*-*F*$^{\text{PhF}}$), −164.6 (m, 4F, *m*-*F*$^{\text{PhF}}$) ppm.

5·triazine. ^{1}H-NMR (300 MHz, CD$_2$Cl$_2$) δ = 9.23 (s, 3H, triazine–*H*), 7.29 (m, 6H, *H*2/*H*3/*H*6/*H*7/*H*10/*H*11), 7.13 (m, 6H, *H*1/*H*4/*H*5/*H*8/*H*9/*H*12), 3.24 (s, 1H, *H*12d), 2.03 (m, 6H, C*H*$_2$CH$_2$CH$_2$B), 1.98–0.87 (m, 42H, overlapping BBN–*H*) 1.36 (m, 6H, CH$_2$C*H*$_2$CH$_2$B) 1.19 (m, 6H, CH$_2$CH$_2$C*H*$_2$B) ppm. ^{11}B NMR (96 MHz, CD$_2$Cl$_2$) δ = 27.8 (s, br) ppm.

6·triazine. ^{1}H-NMR (500 MHz, CD$_2$Cl$_2$) δ = 9.41 (s, 3H, triazine–*H*), 7.22 (m, 6H, *H*2/*H*3/*H*6/*H*7/*H*10/*H*11) 7.09 (m, 6H, *H*1/*H*4/*H*5/*H*8/*H*9/*H*12), 2.96 (s, 1H, *H*12d), 1.95 (m, 6H, C*H*$_2$CH$_2$CH$_2$B), 1.26 (m, 6H, CH$_2$CH$_2$C*H*$_2$B), 0.50 (m, 6H, CH$_2$C*H*$_2$CH$_2$) ppm. ^{11}B-NMR (96 MHz, CD$_2$Cl$_2$) δ = 40.4 (s, br) ppm. ^{19}F-NMR (282 MHz, CD$_2$Cl$_2$) δ = −131.4 (m, 4F, *o*-*F*$^{\text{PhF}}$), −156.1 (m, 2F, *p*-*F*$^{\text{PhF}}$), −162.5 (m, 4F, *m*-*F*$^{\text{PhF}}$).

5·PMe$_3$. ^{1}H-NMR (500 MHz, CDCl$_3$) δ = 7.30 (m, 6H, *H*2/*H*3/ *H*6/*H*7/*H*10/*H*11), 7.09 (m, 6H, *H*1/*H*4/*H*5/*H*8/*H*9/*H*12), 3.53 (s, 1H, *H*12d), 2.04 (m, 6H, C*H*$_2$CH$_2$CH$_2$B), 1.87 (m, 6H, BBN–*H*), 1.64 (m, 24H, BBN–*H*), 1.49 (m, 6H BBN–*H*), 1.11 (d, $^2J_{\text{P,H}}$ = 8.1 Hz, 27H, P(C*H*$_3$)$_3$), 1.00 (m, 6H, CH$_2$C*H*$_2$CH$_2$B), 0.74 (m, 6H, BBN–*H*) 0.58 (t, $^3J_{\text{H,H}}$ = 8.0 Hz, 6H, CH$_2$CH$_2$C*H*$_2$B) ppm. ^{11}B NMR (160 MHz, CDCl$_3$) δ = −4.1 (s, br) ppm. ^{31}P{^{1}H} NMR (202 MHz, CDCl$_3$) δ = −15.6 (s, br) ppm.

5·TrisPhos. ^{1}H-NMR (500 MHz, CDCl$_3$) δ = 7.58 (m, 2H, *o*-SiPh–*H*), 7.43 (m, 3H, *m*-SiPh–*H*, *p*-SiPh–*H*), 7.34 (m, 6H, *H*2/ *H*3/*H*6/*H*7/*H*10/*H*11), 7.14 (m, 6H, *H*1/*H*4/*H*5/*H*8/*H*9/*H*12), 3.57 (s, 1H, *H*12d), 2.12 (m, 6H, C*H*$_2$CH$_2$CH$_2$B), 1.86 (m, 6H, overlapping BBN–*H*), 1.67 (m, 30H, overlapping BBN–*H*), 1.37 (m, 6H overlapping BBN–*H*), 1.26 (m, 6H, CH$_2$C*H*$_2$CH$_2$B), 1.21 (d, $^2J_{\text{P,H}}$ = 6.7 Hz, 6H, SiC*H*$_2$PMe$_2$), 1.11 (d, $^2J_{\text{P,H}}$ = 3.1 Hz, 18H, P(C*H*$_3$)$_2$), 0.95 (t, $^3J_{\text{H,H}}$ = 8.0 Hz, 6H, CH$_2$CH$_2$C*H*$_2$B) ppm. ^{11}B NMR (160 MHz, CDCl$_3$) δ = 9.1 (s, br) ppm. ^{31}P{^{1}H} NMR (202 MHz, CDCl$_3$) δ = −27.2 (s, br) ppm.

Data availability

The data published in this contribution are available as ESI,† submitted with the manuscript.

Crystallographic data have been deposited with the Cambridge Crystal Structure Database (CCDC).

Conflicts of interest

There are no conflicts to declare.

Acknowledgements

References

1 C. J. Pedersen and H. K. Frensdorff, *Angew. Chem., Int. Ed. Engl.*, 1972, **11**, 16–25.

2 (a) W. Uhl, F. Hannemann, W. Saak and R. Wartchow, *Eur. J. Inorg. Chem.*, 1998, 921–926; (b) D. F. Shriver and M. J. Biallas, *J. Am. Chem. Soc.*, 1967, **5**, 1078; (c) F. Schäfer, J.-H. Lamm, B. Neumann, H.-G. Stammler and N. W. Mitzel, *Eur. J. Inorg. Chem.*, 2021, 3265–3271; (d) J. Horstmann, M. Niemann, K. Berthold, A. Mix, B. Neumann, H.-G. Stammler and N. W. Mitzel, *Dalton Trans.*, 2017, **46**, 1898–1913; (e) M. M. Naseer and K. Jurkschat, *Chem. Commun.*, 2017, **53**, 8122–8135.

3 (a) P. Jutzi, J. Izundu, H. Sielemann, B. Neumann and H.-G. Stammler, *Organometallics*, 2009, **28**, 2619–2624; (b) V. C. Williams, W. E. Piers, W. Clegg, M. R. J. Elsegood, S. Collins and T. B. Marder, *J. Am. Chem. Soc.*, 1999, **121**, 3244–3245; (c) C. R. Wade and F. P. Gabbaï, *Z. Naturforsch.*, 2014, **69B**, 1199–1205; (d) H. E. Katz, *J. Org. Chem.*, 1985, **50**, 5027; (e) R. Altmann, K. Jurkschat, M. Schürmann, D. Dakternieks and A. Duthie, *Organometallics*, 1998, **17**, 5858–5866.

4 (a) T. Ooi, M. Takahashi and K. Maruoka, *J. Am. Chem. Soc.*, 1996, **118**, 11307–11308; (b) F. P. Schmidtchen, *Angew. Chem., Int. Ed. Engl.*, 1977, **16**, 720–721, (*Angew. Chem.*, 1977, **89**, 751–752); (c) T. J. Wedge and M. F. Hawthorne, *Coord. Chem. Rev.*, 2003, **240**, 111–128; (d) A. S. Wendji, C. Dietz, S. Kühn, M. Lutter, D. Schollmeyer, W. Hiller and K. Jurkschat, *Chem. – Eur. J.*, 2016, **22**, 404–416.

5 (a) C.-H. Chen and F. P. Gabbaï, *Angew. Chem., Int. Ed.*, 2017, **56**, 1799–1804, (*Angew. Chem.*, 2017, **129**, 1825–1830); (b) H. E. Katz, *J. Org. Chem.*, 1989, **54**, 2179–2183; (c) P. Niermeier, S. Blomeyer, Y. K. J. Bejaoui, J. L. Beckmann, B. Neumann, H.-G. Stammler and N. W. Mitzel, *Angew. Chem., Int. Ed.*, 2019, **58**, 1965–1969, (*Angew. Chem.*, 2019, **131**, 1985–1990); (d) M. Hirai and F. P. Gabbaï, *Angew. Chem., Int. Ed.*, 2015, **54**, 1205–1209, (*Angew. Chem.*, 2015, **127**, 1221–1225).

6 (a) M. F. Hawthorne and Z. Zheng, *Acc. Chem. Res.*, 1997, **30**, 267–276; (b) J. D. Wuest and B. Zacharie, *Organometallics*, 1985, **4**, 410–411; (c) J. D. Beckwith, M. Tschinkl, A. Picot, M. Tsunoda, R. Bachman and F. P. Gabbaï, *Organometallics*, 2001, **20**, 3169–3174; (d) O. Loveday, J. Jover and J. Echeverría, *Inorg. Chem.*, 2022, **61**(32), 12526–12533.

7 (a) A. Schwartzen, J.-H. Weddeling, J. Langosch, B. Neumann, H.-G. Stammler and N. W. Mitzel, *Chem. – Eur. J.*, 2021, **27**, 1821–1828; (b) F. Schäfer, A. Mix, N. Cati, J.-H. Lamm, B. Neumann, H.-G. Stammler and N. W. Mitzel, *Dalton Trans.*, 2022, **51**, 7164–7173; (c) J.-H. Lamm, J. Horstmann, J. H. Nissen, J.-H. Weddeling, B. Neumann, H.-G. Stammler and N. W. Mitzel, *Eur. J. Inorg. Chem.*, 2014, 4294–4301; (d) J. Rudlof, B. Neumann, H.-G. Stammler and N. W. Mitzel, *Z. Anorg. Allg. Chem.*, 2021, **647**, 1967–1972; (e) M. E. Jung and H. Xia, *Tetrahedron Lett.*, 1988, **29**, 297–300.

8 (a) F. Schäfer, B. Neumann, H.-G. Stammler and N. W. Mitzel, *Eur. J. Inorg. Chem.*, 2021, 3083–3090; (b) J. Rudlof, T. Glodde, A. Mix, B. Neumann, H.-G. Stammler and N. W. Mitzel, *Eur. J. Inorg. Chem.*, 2022, e202100842.

9 (a) W. Uhl, A. Hepp, H. Westenberg, S. Zemke, E.-U. Würthwein and J. Hellmann, *Organometallics*, 2010, **29**, 1406–1412; (b) W. Uhl, D. Heller, M. Rohling and J. Kösters, *Inorg. Chim. Acta*, 2011, **374**, 359–365; (c) N. Aders, P. C. Trapp, J.-H. Lamm, J. L. Beckmann, B. Neumann, H.-G. Stammler and N. W. Mitzel, *Organometallics*, 2022, **41**, 3600–3611; (d) N. Aders, J.-H. Lamm, J. L. Beckmann, B. Neumann, H.-G. Stammler and N. W. Mitzel, *Dalton Trans.*, 2022, **51**, 12943–12953.

10 (a) W. Uhl and M. Claesener, *Inorg. Chem.*, 2008, **47**, 4463–4470; (b) J. Tomaschautzky, B. Neumann, H.-G. Stammler, A. Mix and N. W. Mitzel, *Dalton Trans.*, 2017, **46**, 1645–1659; (c) J. Horstmann, M. Hyseni, A. Mix, B. Neumann, H.-G. Stammler and N. W. Mitzel, *Angew. Chem., Int. Ed.*, 2017, **56**, 6107–6111; (d) W. Uhl and M. Claesener, *Inorg. Chem.*, 2008, **47**, 729–735; (e) E. Weisheim, L. Bücker, B. Neumann, H.-G. Stammler and N. W. Mitzel, *Dalton Trans.*, 2016, **45**, 198–207; (f) W. Uhl, A. Hepp, H. Westenberg, S. Zemke, E.-U. Würthwein and J. Hellmann, *Organometallics*, 2010, **29**, 1406–1412; (g) E. Weisheim, C. G. Reuter, P. Heinrichs, Y. V. Vishnevskiy, A. Mix, B. Neumann, H.-G. Stammler and N. W. Mitzel, *Chem. – Eur. J.*, 2015, **21**, 12436–12448.

11 (a) F. P. Gabbaï, A. Schier, J. Riede and D. Schichl, *Organometallics*, 1996, **15**, 4119–4121; (b) J. Chmiel, B. Neumann, H.-G. Stammler and N. W. Mitzel, *Chem. – Eur. J.*, 2010, **16**, 11906–11914.

12 (a) J.-H. Lamm, P. Niermeier, A. Mix, J. Chmiel, B. Neumann, H.-G. Stammler and N. W. Mitzel, *Angew. Chem., Int. Ed.*, 2014, **53**, 7938–7942; (b) J.-H. Lamm, J. Glatthor, J.-H. Weddeling, A. Mix, J. Chmiel, B. Neumann, H.-G. Stammler and N. W. Mitzel, *Org. Biomol. Chem.*, 2014, **12**, 7355–7365.

13 (a) J. L. Beckmann, J. Krieft, Y. V. Vishnevskiy, B. Neumann, H.-G. Stammler and N. W. Mitzel, *Chem. Sci.*, 2023, **14**, 13551–13559; (b) J. L. Beckmann, J. Krieft, Y. V. Vishnevskiy, B. Neumann, H.-G. Stammler and N. W. Mitzel, *Angew. Chem., Int. Ed.*, 2023, **62**, e202310439.

14 J. Tomaschautzky, B. Neumann, H.-G. Stammler and N. W. Mitzel, *Dalton Trans.*, 2017, **46**, 1112–1123.

15 D. Kuck, *Angew. Chem., Int. Ed. Engl.*, 1984, **23**, 508.

16 (*a*) T. Thorwart, D. Roth and L. Greb, *Chem. – Eur. J.*, 2021, **27**, 10422–10427; (*b*) D. Hartmann, T. Thorwart, R. Müller, J. Thusek, J. Schwabedissen, A. Mix, J.-H. Lamm, B. Neumann, N. W. Mitzel and L. Greb, *J. Am. Chem. Soc.*, 2021, **143**, 18784–18793.

17 (*a*) T. Küppers, E. Bernhardt, R. Eujen, H. Willner and C. W. Lehmann, *Angew. Chem., Int. Ed.*, 2007, **46**, 6346–6349; (*b*) J. B. Lambert and Y. Zhao, *J. Am. Chem. Soc.*, 1996, **118**, 7867–7868; (*c*) C. Douvris and O. V. Ozerov, *Science*, 2008, **321**, 1188–1190.

18 (*a*) A. Hermannsdorfer and M. Driess, *Angew. Chem., Int. Ed.*, 2020, **59**, 23132–23136; (*b*) S. A. Weicker and D. W. Stephan, *Chem. – Eur. J.*, 2015, **21**, 13027–13034.

19 (*a*) J. Tomaschautzky, B. Neumann, H.-G. Stammler, A. Mix and N. W. Mitzel, *Dalton Trans.*, 2017, **46**, 1645–1659; (*b*) A. Mix, J.-H. Lamm, J. Schwabedissen, E. Gebel, H.-G. Stammler and N. W. Mitzel, *Chem. Commun.*, 2022, **58**, 3465–3468.

20 D. Kuck, A. Schuster, R. A. Krause, J. Tellenbröker, C. P. Exner, M. Penk, H. Bögge and A. Müller, *Tetrahedron*, 2001, **57**, 3587–3613.

21 M. W. Drover, M. C. Dufuour, L. A. Lesperance-Nantau, R. P. Noriega, K. Levin and R. W. Schurko, *Chem. – Eur. J.*, 2020, **26**, 11180.

22 P. Erdmann, J. Leitner, J. Schwarz and L. Greb, *ChemPhysChem*, 2020, **21**, 987–994.

23 G. Markopoulos, L. Henneicke, J. Shen, Y. Okamoto, P. G. Jones and H. Hopf, *Angew. Chem., Int. Ed.*, 2012, **51**, 12884–12887.

24 Y. Cohen, L. Avram and L. Frish, *Angew. Chem., Int. Ed.*, 2005, **44**, 520–554.

25 Y. H. Zhao, M. H. Abraham and A. M. Zissimos, *J. Org. Chem.*, 2003, **68**, 7368–7373.

26 P. Coppens, *Science*, 1967, **158**, 1577–1579.